

A Survey on Zeolite Synthesis and the Crystallization Process: Mechanism of Nucleation and Growth Steps

Zahra Asgar Pour ¹, Yasser A. Alassmy ²  and Khaled O. Sebakhy ^{3,*} 

¹ Research and Development Department, Kisuma Chemicals, Billitonweg 7, 9641 KZ Veendam, The Netherlands; asgarpour@kisuma.com

² Refining and Petrochemicals Technologies Institute, Center of Excellence for Petrochemicals (Oxford), King Abdulaziz City for Science and Technology (KACST), Riyadh 11442, Saudi Arabia; yalassmy@kacst.edu.sa

³ Laboratory for Chemical Technology (LCT), Department of Materials, Textiles and Chemical Engineering, Ghent University, Technologiepark 125, 9052 Ghent, Belgium

* Correspondence: khaled.sebakhy@ugent.be; Tel.: +32(0)-496764493

Abstract: Zeolites, as a class of crystalline minerals, find a wide range of applications in various fields, such as catalysis, separation, and adsorption. More recently, these materials have also been developed for advanced applications, such as gas storage, medical applications, magnetic adsorption, and zeolitic-polymeric membranes. To effectively design zeolites for such intriguing applications, it is crucial to intelligently adjust their crystal size, morphology, and defect population in relation to crystal perfection. Optimizing these fundamental parameters necessitates a deep understanding of zeolite formation mechanisms, encompassing the thermodynamics and kinetics of nucleation steps as well as crystallite growth. In this review, we discuss the formation of zeolites from this perspective, drawing on recent studies that highlight new achievements in remodeling and modifying zeolite synthesis routes. The ultimate aim is to provide better comprehension and optimize the functionality of zeolites for the aforementioned applications.

Keywords: zeolites crystallization; nucleation mechanism; growth mechanism; crystalline defects; crystal habit; crystal imperfection



Citation: Asgar Pour, Z.; Alassmy, Y.A.; Sebakhy, K.O. A Survey on Zeolite Synthesis and the Crystallization Process: Mechanism of Nucleation and Growth Steps. *Crystals* **2023**, *13*, 959. <https://doi.org/10.3390/cryst13060959>

Academic Editors: Mingyang Chen, Jinbo Ouyang and Kangli Li

Received: 17 May 2023

Revised: 5 June 2023

Accepted: 12 June 2023

Published: 15 June 2023



Copyright: © 2023 by the authors. Licensee MDPI, Basel, Switzerland. This article is an open access article distributed under the terms and conditions of the Creative Commons Attribution (CC BY) license (<https://creativecommons.org/licenses/by/4.0/>).

1. Introduction

The factors governing the crystallization process are important tools to understand the physicochemical properties of a wide range of crystalline materials. Such elements also help us to predict how the crystallization is propagating through the lattice and how to tune the functionality of these materials by controlling the crystallization mechanism [1]. In this context, zeolites, as a class of crystalline materials with a variety of applications (catalysis, sorption, separation, etc.), demonstrate excellent versatility with chemical modifications [2]. However, they are sometimes very sensitive to adding new particularities to their existing specifications, meaning that their formation chemistry has some boundaries; and outside of those areas, pure phase cannot exist [3]. For example, high degrees of delicacy should be considered for the synthesis of zeolite using some metals such as Ti (Titanium), Sn (Tin), Zr (Zirconium), or Hf (Hafnium), in the presence or in the absence of Al. The insertion of these atoms inside the framework of zeolites is tough work unless some additional components are added to the primary suspension to assist the crystallization step [4,5]. Namely, we can use special and sometimes expensive structure-directing agents (SDAs) or environmentally noxious mineralizers, such as HF, to incorporate such metals into the framework [6,7]. The conventional synthesis of zeolitic materials containing the above-stated elements is troublesome since their atomic radius is larger, while their chemical reactivity is remarkably different and mainly slower compared to Si and Al atoms; therefore, they can form amorphous metal oxide phases instead of being grafted into the

zeolitic framework. The formation of amorphous phases, which has been observed by the introduction of such metals into the synthesis mixture, can also decrease the surface area of the final material due to the blockage of the porous network [4].

In addition to the compositional adjustment, crystal morphology and dimensions of zeolitic particles are important parameters influencing the functionality of zeolites for novel applications [8]. The so-called “crystal habit” generates a wide range of geometric appearances for crystallites, such as acicular, tabular, or striated, as specified by crystal aspect ratios (e.g., length, width, and thickness) plus numbers of crystal planar surfaces [9]. The crystal habit of formed zeolite is influenced by synthesis parameters, such as the type of inorganic species (e.g., heteroatoms as stated above), type and amount of organic SDAs, synthesis temperature, and presence of impurities. So, the final morphology is the outcome of the interplay between these different parameters; and thus, based on the various and empirical combinations of these factors, a wide range of zeolite particles, from nano-crystalline to gigantic crystals (centimeter range or higher in magnitude) as well as equi- or multidimensional crystalline zeolites, can be crafted by the engineering of crystal habits [9,10].

The type and population of crystalline defects are other pivotal properties influencing zeolites physicochemical properties. Advancing zeolite functionality beyond the state-of-the-art properties is directly related to the engineering of crystals defects. In zeolitic crystalline domains, four different types of defects are known: point defects (e.g., missed or replaced atoms in the connection parts to the lattice), line defects (e.g., dislocated fringes), surface defects (e.g., twin boundaries), and volume defects (e.g., voids) [11]. Generally, defect-free crystals are good candidates for membrane application whereas highly-defective crystals are preferred for catalysis [12,13]. For instance, by application of HF as a mineralizer during the hydrothermal synthesis, defect-free zeolites are obtained; in contrast, the top-down post-synthesis techniques introduce different types of defects into the zeolite structure, such as point, surface, and volume defects that are filled or occupied with functional groups (e.g., hydroxyl group) in order to stabilize the defects. In this condition, the evolution of crystalline phase structurally deviates from ideal and defect-free crystal formation. Furthermore, the zeolitic crystalline defects are classified into intrinsic and extrinsic defects. The extrinsic defects can be controlled by altering synthesis conditions; however, the intrinsic defects, which originated from the inherent chaotic behavior of crystal constituents, generate misoriented domains in the nano-range with irregular atoms arrangements. Due to the complexity of the formation, the control of intrinsic defects is not simple and they cannot be suppressed completely [14]. Such defects can be extended to larger domains and introduce intergrown or twin structures [15]. Although the microscopic techniques are not the focus of this review, however, by using TEM (Transmission Electron Microscopy) and AFM (Atomic Force Microscopy) in both in situ and ex situ operation modes, significant progress has been made in the field of zeolite nucleation and growth step and this has increased our knowledge about zeolite crystallization. Nevertheless, studies are still going on and our insight does not yet fully cover unknown aspects of this subject [10,16]. A better understanding of zeolite nucleation, along with growth mechanisms and structural defects, helps us to fundamentally realize different underlying crystallization routes, formed morphology, and surface growth stability (i.e., stable versus meta-stable growth) [17]. Therefore, they are the main core of this review and will be discussed in the coming sections.

2. Nucleation Mechanism

Nucleation is the first step of crystal formation that initiates by atoms accumulation in a small cluster inside the primary suspension. Dissolved species tend to form a quasi-solid phase, which is called nuclei, and likely contribute to the irreversible formation of the ultimate crystalline product through smart selections of crystallization conditions [18–22]. It also indicates that inappropriate conditions can make this process reversible and the formed clusters can be redissolved in the mixture of precursors. The motive force, which is exerted

on the suspended particles to begin the nucleation, is called supersaturation and acts as chemical potential between the dissolved species and consequently, forms a quasi-solid phase. In fact, the discrepancy between the actual concentration of zeolite precursors and the concentration at a solubility equilibrium at a certain temperature is known as supersaturation. As a possible effect, elevating the temperature can increase the entropy and chemical potential for a given synthetic system and, thus, facilitate the supersaturation condition in favor of the primary nucleation step [23]. However, it should be noted that increasing the temperature does not always positively affect the nucleation step and may suppress the nucleation by assisting the formation of different phases that are not thermodynamically desired for the nucleation step. In contrast, if the system shifts under supersaturation condition, clusters are dissolved in the primary solution [24]. Thermodynamically, two parameters govern how and at what speed the nucleation step is proceeding: (i) the difference in the total free energy of the system between the two final states (i.e., dissolved particles as State 1 and formed cluster as State 2, which is known as a bulk term; and (ii) the interaction between the solid centers and suspension phase at the interfaces, which is known as a surface term [24]. By realizing this, the nucleation rate can be altered by setting the supersaturation condition, indicating the higher the supersaturation, the faster the rate of nucleation, and the smaller the crystal size distribution. There is a threshold amount for supersaturation (i.e., so-called critical supersaturation zone, also characterized as the meta-stable zone); This is a region which above it, the nucleation occurs exponentially [25], yet, very close to this region, the crystal growth dominates the negligible nucleation and only a few large crystals are formed. In other words, when the system shifts to a critical supersaturation condition, nucleation occurs in a short time and stops quickly because the process reaches a phase that is incapable of forming crystals [26,27]. Furthermore, in the critical supersaturation region, the formed nuclei possess a critical radius which below this radius nuclei dissolve; in contrast, above it, nuclei can reduce the formation Gibbs energy and further grow [16]. The primary nucleation classically occurs via two different pathways: (i) homogeneous nucleation in a pure phase, which uniformly grows from the parent phase via local fluctuations; or (ii) heterogeneous nucleation at low supersaturation, which occurs by adding seeds or in general in the presence of impurities [19–22]. However, both types of nucleation assists lowering the surface energy to the possible negative value [28]. Despite these routes and regardless of which one is the cause of primary nucleation, secondary nucleation is the result of several dynamic interplays in the nucleating medium as well as surface interactions eventuating in polycrystalline breeding. For instance, the separation of extremely small particles from the surface of clusters or crystals, due to the collision of particles, abrasion, or shear stress, is a known factor causing the second nucleation step [29]. The mechanism of nucleation and the different steps that happen in the course of time are represented in Figure 1. By inversing conditions, redispersion occurs and agglomerates are dissolved in the solution. The primitive particles that are initially formed in the basic medium construct a primary amorphous phase; however, over time, the secondary amorphous phase is formed, which is characterized by short-range orders. Due to this new ordering, this phase is different from the primary amorphous phase. By aging and heating under autogenous pressure, secondary phase is gradually rearranged and further grow with a repetitive order and is finally transformed into crystalline zeolite particles.

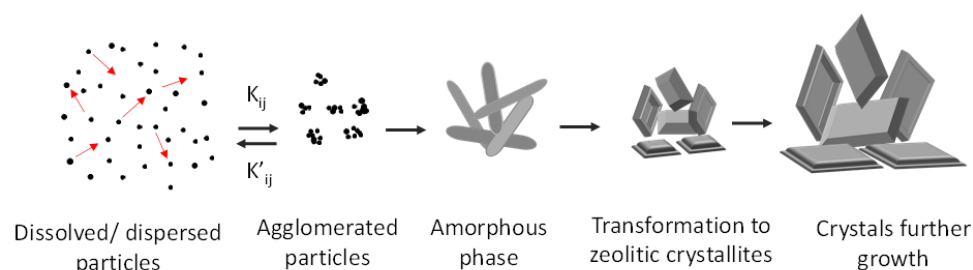


Figure 1. Schematic illustration of nucleation and growth mechanism. Discrete and ultramicroscopic

colloidal nuclei are agglomerated after certain period of induction. The agglomeration rate constant is (K_{ij}). The process further proceeds to produce dimer, trimer, and finally polymeric particles. If the reaction conditions, such as the temperature, polarity of solvents, or rate of stirring, are not selected properly, the agglomerates redissolve in the mixture with a dissolution rate constant equal to (K'_{ij}). In such cases, precipitated particles, which are still in the meta-phase are not fully stabilized to be completely a solid phase, and thus can be gradually re-dispersed in the suspension.

In another classification, the nucleation step is divided into instantaneous and progressive nucleation (Figure 2). Instantaneous nucleation occurs promptly and grows fast while, with progressive nucleation, the nuclei continue to develop and increase during the deposition process at a continuous rate [30].

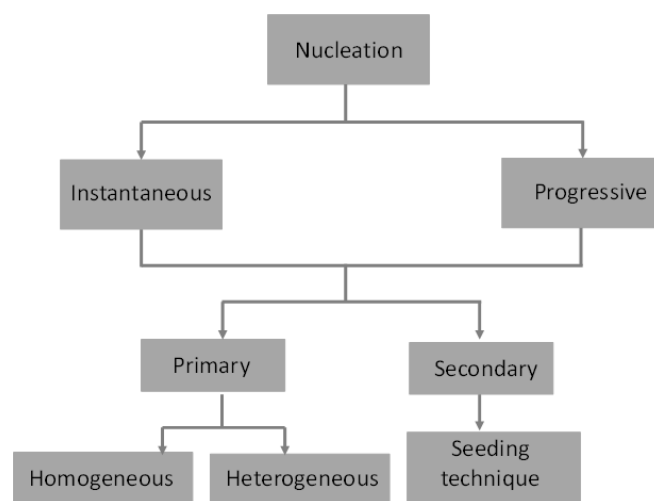


Figure 2. The chart of different types of nucleation.

3. Growth Mechanism

Crystal growth initiates via atom migration from the suspension of precursors toward the forming crystalline surface and continues with atom attachment and rearrangement inside the crystalline lattice. It is worth mentioning that when the growth step reaches a steady state condition, the supersaturation levels off and next, decreases because nutrients are gradually consumed during the crystal growth. Cluster growth can be assumed to happen initially through Ostwald ripening and further proceeds with the gradual aggregation of small species [31]. From the classical point of view, zeolite crystal growth is a surface phenomenon including several sub-steps, the slowest of which is kinetically controlling the growth process. In this respect, the growth occurs on the surface and subsequently spreads toward the edges and kinks of the crystal unit [32,33]. However, it should be noticed that due to the presence of an organic structure directing agent (SDA) in the synthesis of zeolites and presence of some other elements (e.g., Na, K, etc.), the growth step is a complex process and its reaction mechanism is not yet fully clear. For instance, the interaction between inorganic precursors and the organic phase (SDA) impacts both the crystallization process and crystal size [1,34]. Recently and in contrast with the classical surface growth mechanism, a truly reverse zeolite growth has been reported via tuning the concentration of SDA [34]. It has been visualized by electron microscopic techniques that the growth step is conducted by the transformation of a spherical amorphous surface into a crystalline surface. The study of the inner structure of these spheres by microscopic analysis also disclosed that following the surface transformation, crystallization propagates toward the central part of the spherical aggregates [34]. Although the key factors directing reverse growth are still elusive, in this work, a study on the amount of SDA showed that there is a critical value for SDA quantity; below that, the classical crystallization determines the growth pathway while, using higher amounts of SDA, the reverse crystal growth is the dominant

mechanism. As discussed above, this study once more demonstrates the importance of adjusting the synthesis parameters to better control the growth mechanism [34]. Another example of reverse zeolite growth is the synthesis of zeolite crystallites inside the polymeric scaffold. Due to the host–guest interactions and confined impacts of the polymer, the crystallization starts at interfaces and proceeds toward the inner parts of solid inorganic phase, indicating the reverse route of growth [5,35]. In addition, the presence of amorphous phases, along with the generation of more than one zeolitic phase in the case of polymer application, verifies that the chemistry of polymers alters the mechanism of the growth step compared with the classical approach [5,35–37]. Altogether, the reverse zeolite growth is a complementary mechanism to the classical mechanism and shows that, instead of the layer-by-layer growth of crystalline units, the aggregation of precursors can change the crystallization route in which the large amorphous sheets or polycrystalline particles can be transformed to a homogenized crystalline phase by crystallization/ recrystallization of the surface. Such behavior generates a crystalline shell which can further extend the crystallinity toward the core area [38]. Using this mechanism, interesting morphologies, such as core-shell or hollow structures, can be obtained [38]. Apart from the effects of SDA and polymers, the zeolite growth step is also related to several parameters, such as temperature, primary mixture composition, aging time, and stirring modes [5,39,40]. Furthermore, it has been frequently reported that the zeolite growth rate is linear during the majority of the crystallization step.; By means of density functional theory, it has been shown that oligomerization of species (as the first step of growth) is thermodynamically an exothermic step and the amount of released heat for zeolites samples is higher than the silicate analogs. The presence of Na^+ is another factor which affects the growth step by favoring the formation of linear oligomers rather than cyclic oligomers [32,41]. In a recent study, the effect of temperature has been also investigated for MER topology (zeolite W) and it has been revealed that temperature alters the crystallization growth mechanism [42]. Synthesis at 90 °C in a highly supersaturated solution produced zeolite W, which developed through birth and spread growth (see below); whereas, synthesis at 175 °C demonstrated a spiral growth (see below) of zeolite W crystallites. These observations resulted in the conclusion that the higher the temperature, the more elongated the crystal morphology [42]. The temperature dependence of the growth step was further studied by an analysis of two factors at both temperatures: supersaturation condition and Al atoms evolution during the crystallization. By suggesting an Arrhenius type of equation for the crystallization step as a function of the reactive surface, activation energy, and temperature (see Ref [42]), it was found that at higher temperatures (175 °C), lower degrees of supersaturation is generated and, consequently, the kinetics of the synthesis and morphology of the crystallites during the growth step differs from the ones formed at 90 °C. However, the growth mechanism and crystal morphology were found to be independent of Al concentration as, in both cases, the synthesis starts with high Al content and Al is consumed gradually over time [42]. In Table 1, a summary of examples of different possible morphologies for different zeolitic frameworks is presented.

Table 1. Examples of zeolite with identical frameworks and different morphologies.

Zeolitic Framework	Example	Morphology	Synthesis Conditions	Ref.
MER	Zeolite W	Lamellar cubes	90 °C	[42]
		Elongated cubes	175 °C	[42]
MFI	ZSM-5	Coffin shape Microspheres	Conventional In the presence of carbon nanotubes	[5] [43]
BEA	Zeolite Beta	Stacking structure Uniform prism-like crystals	Conventional F [−] medium	[5] [44]
FAU	Zeolite Y	Octahedrons Microspheres	Conventional Seeding technique	[5] [45]
MOR	Mordenite	Fiber bulky sphere, circular pie, flat prism, hexagonal star-like prism, and ellipsoid	Conventional acid-catalyzed hydrolysis and tetraethyl ammonium hydroxide as a template	[46] [47]

Developing the knowledge about zeolite growth mechanisms has shown to be very fruitful for the construction of new and innovative structures, such as chiral pores, extra-large pores, and extremely complex framework topologies [48,49]. On this subject, several surface growth models have been theorized in past decades, such as monoatomic layer growth as a model in which terraces and vacancies on the layer formation step demonstrate a less ideal and more practical mechanism of growth [32]. Furthermore, when the nucleation rate exceeds the time needed for covering the crystal surface, the growth mechanism deviates from the monolayer state and new nuclei grow on top of previous ones. Such behavior causes multilayer growth, which smoothly develops a crystalline surface. This mechanism is also known as birth and spread and results in the surface homogeneous evolution [50].

The growth step is highly promoted at high supersaturations, which are thermodynamically regions with high levels of potency required to overcome energy barriers for 2D nuclei formation. However, low supersaturations are also capable of generating nuclei and fostering crystals. The ability of crystallization in these domains originated from the presence of dislocations, which can cut off the crystalline surfaces and gradually construct more steps on the crystal surfaces (e.g., the formation of remarkably smaller surfaces which possess different heights compared with the primary surface). This growth behavior of crystalline surfaces removes the necessity for 2D nucleation [51]. Nonetheless, the second and next steps should dimensionally grow beyond the critical diameter (i.e., $2r_{\text{critical}}$) to make the stepping process thermodynamically feasible [42,51]. In practice, lower supersaturations alter the growing behavior of the crystalline surface, which digresses from birth/spread growth type and shifts to spiral growth format with self-stepping patterns around dislocation centers [42,51]. This type of crystal growth also produces smooth crystalline surfaces [51]. Spirally-growing surfaces can be interlaced and produce more complicated surface morphologies [52]. Such disordered growing patterns are built by the successive stacking of growing layers. As these layers are positioned diversely, leads to inhomogeneity during surface development [53–55]. Here, the important factor, which produces anisotropic crystalline faces, is the different rates of formation and growth of step units, which is faster in some directions and slower in some other routes [53–55].

As mentioned above, supersaturation can directly affect the crystal growth patterns [51,56–58]. At lower supersaturations, smooth surfaces are developed by a spiral type of growth while increasing supersaturation replaces the spiral pattern with birth/spread growth, which still develops smoothly. Indeed, birth and spread growth is achievable after passing the critical supersaturation region for 2D nucleation in the phase diagram. In both domains, crystals grow with polyhedral morphologies and flat faces. In contrast, highly concentrated supersaturations produce rough surfaces with the adhesive type of growth. Generally, increasing supersaturation increases the possibility of adhesive growth with higher degrees of irregular interfaces, such as fractal, spherical, and other complex morphologies [51,56–58].

Apart from the study of growth phenomenon on microscopic scale, zeolitic-phase formation can be systematically controlled during the synthesis and by means of precise setting of the experimental parameters. In this context, the crystalline particles in the nanometer range are obtained by restricting the growth step of conventional micron-size crystals [58]. For instance, the type and amount of SDAs [1], aging time [5], crystallization time, and temperature [5] can be regulated to produce fine crystalline particles [58]. Increasing the amount of SDA and lowering the temperature of the synthesis in the absence or deficit of Na^+ [1] or the application of hard templates, such as porous carbons or polymers, can prevent crystal growth through suppressing nanoparticle aggregation or confinement effects. In addition, 2D zeolites are an interesting family of zeolites which are specified by their lamellar crystalline and porous structure [59,60]. These zeolites are obtained by the growth and following assembly of nano-layers in one particular dimension which is originated from weak or the absence of covalent bonds between their layers. In this class

of zeolites, the stacking sequence can be modified, which enables scientists to synthesize diverse structures [59,60]. 2D zeolites are interesting materials because they produce better accessibility with enhanced mass transfer to the active sites, which are desired properties for catalysis and adsorption processes. Therefore, their synthesis method and growth mechanism are described briefly as the supplementary part of this section. From synthesis point of view, 2D zeolites can generally be prepared using three different techniques: (i) by the application of lamellar precursors and preserving their 2D properties during the synthesis; (ii) by a restricted growth mechanism during the crystallization, which is feasible through employing a particular surfactant acting as template for the formation of 2D and layered structure; and (iii) by a top-down post-synthesis technique [61,62]. Among these techniques, the second method is interesting in terms of crystallization growth step in line with the subject of this review. The role of surfactant is similar to organic SDAs for synthesis of 3D zeolites, for example, pores filling and structural stabilizing effects [1]. However, another task of specifically designed surfactants for 2D zeolites is to produce a lamellar structure, which is remarkably different from the SDAs applied to produce 3D zeolites. For the synthesis of 2D zeolites with a layered structure, the surfactant properties, such as the degree of hydrophobicity, size of the organic linker, and the hydrophilic part of the molecule, should be designed smartly. The hydrophilic part of the surfactant assists zeolite crystallization, while the long hydrophobic chains prevent the further growth of crystals, and thus a stacking structure is produced [62].

4. Types of Structural Defects in Zeolites

Crystal defects are built by different structural and lattice imperfections in zeolite domains. Stacking faults and complex intergrown subunits are the two most common defects in zeolitic frameworks [63–65]. In the context of stacking faults, zeolite Beta (BEA framework) is an interesting example because of the presence of three polymorphs with different stacking faults (i.e., chiral polymorph A, achiral polymorph B, and polymorph C) as well as having a lot of hydroxyl groups in its structure. The high population of silanol groups in the framework of zeolite Beta has been explained by the occurrence of two different stacking faults at the same layer, which cannot be connected at edges or boundaries; therefore, they create too many abnormal pores with open bonds which end with terminal silanol groups [63]. Defects of zeolite Beta have been visualized by HRTEM (High-Resolution TEM); and based on a layer-by-layer mechanism, such defects have been proposed as main defects during the growth of this zeolite. However, the growth can happen in different sections of the same layer with various and heterogeneous stacking vectors as well [64]. The TEM images of zeolite Beta and zeolite Y are illustrated in Figure 3A and Figure 3B, respectively. Zeolite Beta contains high amounts of layered stacking faults compared with Zeolite Y and possesses significantly more edges and fringes in shorter distances, which require to be terminated with hydroxyl groups and such need makes the high density of OH groups explainable [63]. To address intergrowth defects, zeolite T is an interesting example because it is the outcome of the structural intergrowth of erionite (ERI) and offretite (OFF). Here, the twelve-member ring offretite pores can be blocked by the intergrowth of the eight-member ring erionite. Therefore, erionite intergrowth generates more levels of malformations and irregularities. However, the degree of intergrowth can be adjusted by tuning the synthesis parameters to give rise to optimal properties [54]. As another example for zeolitic defects, the study of the large crystals of zeolite analcime with polyhedral morphology using single crystal XRD has shown that the low crystallinity of this material is due to the presence of a lot of structural defects, which is attributed to the aggregation of nanoplatelets, and consequently the formation of clusters instead of the continuous and pure growth of crystallites [58].

From a synthetic point of view, thermal treatment (calcination at elevated temperatures), elemental extraction using acid or base solutions, and steaming can also introduce defects in zeolite network; they are considered defects that are structurally generated in as-

synthesized zeolites but are not considered inherent defects (i.e., those which are generated simultaneously during the building of zeolitic crystals) [66].

From a structural point of view, defects are divided into four types: volume defects, surface defects, line defects, and point defects. In general terms, volume defects, as stated above, are created due to the lack of chemical bonds, resulting in the formation of T-OH bonds. Volume defects are also known as bulk defects and can also be produced by missing tetrahedrally coordinated T atoms, and lead in the formation of voids in the structure [66,67]. Some factors can enhance the generation of these defects during the zeolite synthesis, such as contact with water molecules, the presence of heteroatoms (e.g., Ti), the presence and type of organic template, or dual templating [67–70]. Bulk defects also depend on the synthesis parameters and by the well-adjusting conditions for each zeolite sample, the density of defects can be reduced or the grain boundaries can be healed. In line with these facts, some frameworks are more prone to bulk defects than others [10,67–69]. The surface type of defects can be generated during the growth at twin boundaries and are assumed to be the major mechanism of growth resulting in the densification of polycrystalline zeolites, such as faujasite (FAU framework) [71]. In this type of defect, the growth takes place at the boundary of two crystals, which could link the crystals together and produce disorders that are known as surface defects [71]. Surface defects are mainly observed in the absence of seeding techniques and owing to the linkage between the crystals, the original morphology of crystals are changed in the surface defects regions. In the case of the faujasite framework, the hexagonal geometries of the crystallites are altered and more irregular shapes are constructed [71]. The line defects in zeolites are formed due to the dislocated fringes and, thus, can change the stacking orders [72]. They can also be formed by the dissemination of point defects with a 2D pattern in the framework system. Point defects are created due to a missing atom in the connecting regions [72–74]. The point defects can be distributed in the network and change the textural properties of the framework massively. A disrupted point can propagate and develop a disrupted region. These defects are responsible for both line and bulk defects. Considering the 2D or 3D direction of spreading defects, they will form large areas of void spaces representative of bulk defects or linear areas indicating the line defects [72–74].

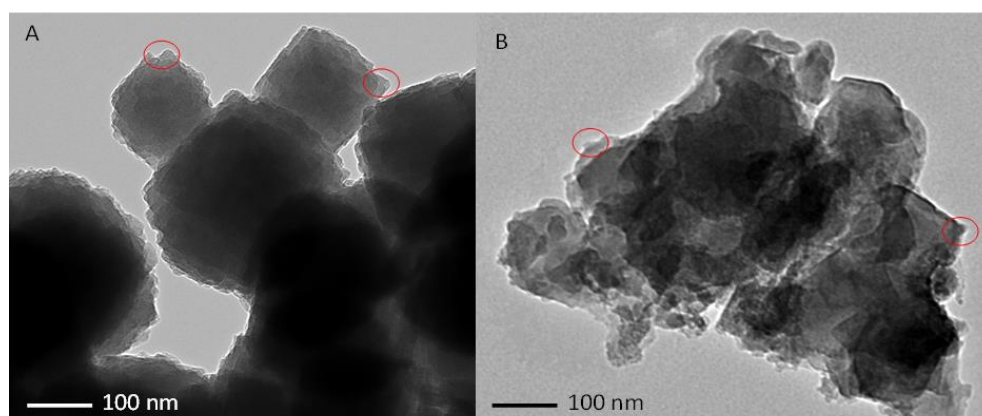


Figure 3. TEM image of (A) zeolite Beta and (B) zeolite Y crystalline particles. Two edges of crystallites with morphological dislocation are shown with red circles.

The structural defects, as far as we discussed, alter the physicochemical properties of crystals in comparison with the case of ideal crystal perfection. However, such defects are caused by the intrinsic behavior of forming crystals and due to the crystal habits, they are inevitable. Furthermore, despite their presence, they are controllable and can be adjusted to be reduced, healed, or optimized for a given demand [75]. For instance, organic SDA-free synthesis, which is limited to a narrower range of Si/Al for each framework, can change the crystal structure as well as the crystal habits because these properties are functions of the molar composition (e.g., Si, Al, OH), temperature of synthesis, and time of crystallization.

Using a specific experimental setting for these parameters, the crystal habit, morphology, as well as type, and population of defects can be modified. To exemplify these alterations, one protocol is the use of acid treatment, by which higher degrees of volume and surface defects are inserted into the framework. These centers can accept open metals or hydroxyl groups as active centers for catalysis. Another example is the application of modifiers, such as polymers, which can provide crystallographic faces for linkage to the surface of crystals and so can hamper crystal growth. The growth suppression can be also caused by the adsorption of functional species on terraces, which works to diminish 2D-layer nucleation, or by their attaching to the steps to prevent the precursors to further bind to kinks and hence can decrease the crystallization rate via inhibiting the growth of crystal step units [75,76]. It has been reported that for MFI zeolite, the preferential location of defects is close to the terminal methyl group of the longer alkyl chain. Furthermore, MFI samples prepared by non-symmetric methyl tri-*n*-butyl-ammonium hydroxide (MeTrBA), were prone to defects in the sinusoidal channels; MFI samples prepared by tetra propylammonium hydroxide (TPA) generated defects which were casually distributed in all channels [76]. Although the research on zeolite crystal defects and the origin of their formation is an ongoing study, the advancement obtained in macroscopic techniques has been notably useful for elucidating the unknown aspects of defect formation. Using some macroscopic techniques, such as AFM (Atomic Force Microscopy), HRSEM (High-Resolution Scanning Electron Microscopy), and Confocal Microscopy, as well as spectroscopic techniques, such as NMR (Nuclear Magnetic Resonance), the knowledge of zeolite nucleation, growth, and defect formation, have been developed significantly in the past years. Although the measurement techniques were not the core of this review, it should be emphasized that they can be widely used to support our findings about the fundamental aspects and chemistry of zeolite formation.

5. Recent Advances in the Modeling of Zeolite Crystallization Using Machine Learning

More recently, machine learning and computational statistics have been applied to zeolite science [77]. The target is to use machines for predicting the quantitative output of synthesis pathways, providing a greater ability to predict zeolite yield and performance [77,78]. In this regard, different mathematical models, such as linear regression, ridge regression, regression tree, random forest, XGBoost, and artificial neural network models, can be employed [77]. Using these models by means of introducing synthesis variables as input, the model versatility and machine ability have been assessed. The promising results of such modeling for zeolite LTA indicated that machine learning in combination with experimental techniques can be used as a tool in zeolite science [77]. In addition, computational statistics were used for extracting data, including synthesis information and trends from zeolite journal articles, to predict different features of Germanium-containing zeolites, such as framework density [78]. Machine learning has also been employed for the prediction of the zeolitic framework [79]. By developing a nine-dimensional feature vector consisting of novel topological descriptors designed by computational geometry methods, a tool for the accurate prediction of a new framework has been modeled by the integration of the above-stated mathematical model with a series of physicochemical properties of zeolite crystals [79]. This study showed that such a technique can be useful for precise prediction of zeolitic framework [79]. Interestingly, machine learning is a helpful technique that can be used to explore the new aspects of thermodynamics and kinetics of zeolite formation [80]. It enabled researchers to evaluate the effect of SDAs, Si/Al ratio, pH, and other elements, such as phosphorous, on zeolite phase formation, stability, and type of growth (stable vs. meta-stable energy zones), and also proved that the alkaline pH is a suitable medium for the Si–O–Al bonding [80]. The machine learning technology is developing quickly and those case studies that we discussed above are only some examples of several attempts that have been conducted in this field to make zeolite science (e.g., synthesis, kinetics, thermodynamics, framework formation, etc.) more explicit and predictable for the highly rational and optimal design of zeolites in the future.

6. Conclusions

Although the fundamentals of zeolite chemistry and structural properties have been studied for a long time and zeolites have established their place and rank in several fields, the requirement for their optimization for current and advanced applications is always necessary [81–84]. The number of studies that are released every year, including the new findings about the characteristics of zeolites, is the evidence to certify such a need. In this regard, crystal nucleation and growth are interesting aspects of zeolite synthesis that have been continuously investigated in the past years to understand, in more detail, their mechanisms of formation and growth. In addition, the kinetics, and thermodynamics of zeolite crystallization play an important role in the formation of the final zeolitic phase and, in merging with the knowledge of chemical synthesis, provide controllable routes for tailoring the physicochemical properties of zeolites. The combination of these subjects is also a useful tool that enables us to interpret new achievements, craft new zeolitic frameworks, and explore unknown observations, such as types of growth or structural faults. Although the fundamentals of nucleation and growth phenomena are also applicable to zeolite crystallization, zeolites are porous materials and their synthesis generally requires the application of organic SDAs. The interactions of organic species with inorganic precursors also make zeolite synthesis more complicated than other inorganic metal oxides. To elucidate different aspects of zeolite synthesis, the development of non-classical nucleation pathways that can explain the complexities of zeolite formation seems unavoidable. Employing new approaches that can improve the efficiency of zeolite syntheses, such as short time of preparation, lower amount of waste, and restricted use of environmentally noxious materials, implies developing zeolite synthesis science through the application of experimental approaches, such as microscopic techniques, in combination with computational simulations. In this review, the goal was to argue the process of formation of a zeolite (i.e., nucleation and crystallization) and we attempted to translate these phenomena into a versatile but straightforward discussion that is applicable for researchers from different backgrounds.

Author Contributions: Conceptualization, Y.A.A. and Z.A.P.; methodology, Y.A.A.; formal analysis, K.O.S.; investigation, Z.A.P.; resources, writing—original draft preparation, Z.A.P.; writing—review and editing, K.O.S.; visualization, Y.A.A.; supervision, K.O.S. All authors have read and agreed to the published version of the manuscript.

Funding: This research received no external funding.

Data Availability Statement: Not applicable.

Acknowledgments: Khaled O. Sebakhy thanks the Laboratory for Chemical Technology (LCT), University of Ghent, Belgium.

Conflicts of Interest: The authors declare no conflict of interest.

References

1. Asgar Pour, Z.; Sebakhy, K.O. A Review on the Effects of Organic Structure-Directing Agents on the Hydrothermal Synthesis and Physicochemical Properties of Zeolites. *Chemistry* **2022**, *4*, 431–446. [\[CrossRef\]](#)
2. Asgar Pour, Z.; Abduljawad, M.M.; Alassmy, Y.A.; Cardon, L.; Van Steenberge, P.H.; Sebakhy, K.O. A Comparative Review of Binder-Containing Extrusion and Alternative Shaping Techniques for Structuring of Zeolites into Different Geometrical Bodies. *Catalysts* **2023**, *13*, 656. [\[CrossRef\]](#)
3. Pilar, R.; Moravkova, J.; Sadovska, G.; Sklenak, S.; Brabec, L.; Pastvova, J.; Sazama, P. Controlling the competitive growth of zeolite phases without using an organic structure-directing agent. Synthesis of Al-rich* BEA. *Microporous Mesoporous Mater.* **2022**, *333*, 111726. [\[CrossRef\]](#)
4. Asgar Pour, Z.; Boer, D.G.; Fang, S.; Tang, Z.; Pescarmona, P.P. Bimetallic Zeolite Beta Beads with Hierarchical Porosity as Brønsted-Lewis Solid Acid Catalysts for the Synthesis of Methyl Lactate. *Catalysts* **2021**, *11*, 1346. [\[CrossRef\]](#)
5. Asgar Pour, Z.; Koelewijn, R.; El Hariri El Nokab, M.; van der Wel, P.C.; Sebakhy, K.O.; Pescarmona, P.P. Binder-free Zeolite Beta Beads with Hierarchical Porosity: Synthesis and Application as Heterogeneous Catalysts for Anisole Acylation. *ChemCatChem* **2022**, *14*, e202200518. [\[CrossRef\]](#)

6. Cambor, M.A.; Corma, A.; Perez-Pariente, J. Synthesis of titanoaluminosilicates isomorphous to zeolite Beta, active as oxidation catalysts. *Zeolites* **1993**, *13*, 82–87. [\[CrossRef\]](#)
7. Van der Waal, J.C.; Lin, P.; Rigutto, M.S.; Van Bekkum, H. Synthesis of aluminium free titanium silicate with the BEA structure using a new and selective template and its use as a catalyst in epoxidations. In *Studies in Surface Science and Catalysis*; Elsevier: Amsterdam, The Netherlands, 1997; Volume 105, pp. 1093–1100. [\[CrossRef\]](#)
8. Li, S.; Li, J.; Dong, M.; Fan, S.; Zhao, T.; Wang, J.; Fan, W. Strategies to control zeolite particle morphology. *Chem. Soc. Rev.* **2019**, *48*, 885–907. [\[CrossRef\]](#)
9. Maldonado, M.; Oleksiak, M.D.; Chinta, S.; Rimer, J.D. Controlling crystal polymorphism in organic-free synthesis of Na-zeolites. *J. Am. Chem. Soc.* **2013**, *135*, 2641–2652. [\[CrossRef\]](#)
10. Palčić, A.; Moldovan, S.; El Siblani, H.; Vicente, A.; Valtchev, V. Defect sites in zeolites: Origin and healing. *Adv. Sci.* **2022**, *9*, 2104414. [\[CrossRef\]](#)
11. Medeiros-Costa, I.C.; Dib, E.; Nesterenko, N.; Dath, J.P.; Gilson, J.P.; Mintova, S. Silanol defect engineering and healing in zeolites: Opportunities to fine-tune their properties and performances. *Chem. Soc. Rev.* **2021**, *50*, 11156–11179. [\[CrossRef\]](#)
12. Abate, S.; Barbera, K.; Centi, G.; Lanzafame, P.; Perathoner, S. Disruptive catalysis by zeolites. *Catal. Sci. Technol.* **2016**, *6*, 2485–2501. [\[CrossRef\]](#)
13. Wenten, I.G.; Dharmawijaya, P.T.; Aryanti, P.T.P.; Mukti, R.R. LTA zeolite membranes: Current progress and challenges in pervaporation. *RSC Adv.* **2017**, *7*, 29520–29539. [\[CrossRef\]](#)
14. Qin, Z.; Hafiz, L.; Shen, Y.; Van Daele, S.; Boullay, P.; Ruaux, V.; Gilson, J.-P.; Valtchev, V. Defect-engineered zeolite porosity and accessibility. *J. Mater. Chem. A* **2020**, *8*, 3621–3631. [\[CrossRef\]](#)
15. Wu, Q.; Luan, H.; Xiao, F.S. Targeted synthesis of zeolites from calculated interaction between zeolite structure and organic template. *Natl. Sci. Rev.* **2022**, *9*, nwac023. [\[CrossRef\]](#)
16. Choudhary, M.K.; Jain, R.; Rimer, J.D. In situ imaging of two-dimensional surface growth reveals the prevalence and role of defects in zeolite crystallization. *Proc. Natl. Acad. Sci. USA* **2020**, *117*, 28632–28639. [\[CrossRef\]](#)
17. Lupulescu, A.I.; Rimer, J.D. In situ imaging of silicalite-1 surface growth reveals the mechanism of crystallization. *Science* **2014**, *344*, 729–732. [\[CrossRef\]](#)
18. Cundy, C.S.; Cox, P.A. The hydrothermal synthesis of zeolites: Precursors, intermediates and reaction mechanism. *Microporous Mesoporous Mater.* **2005**, *82*, 1–78. [\[CrossRef\]](#)
19. Jain, R.; Mallette, A.J.; Rimer, J.D. Controlling nucleation pathways in zeolite crystallization: Seeding conceptual methodologies for advanced materials design. *J. Am. Chem. Soc.* **2021**, *143*, 21446–21460. [\[CrossRef\]](#)
20. Pollens, N.; Doppelhammer, N.; Asselman, K.; Thijs, B.; Jakoby, B.; Reichel, E.; Taulelle, F.; Martens, J.; Breynaert, E.; Kirschhock, C.E.A. A zeolite crystallisation model confirmed by in situ observation. *Faraday Discuss.* **2022**, *235*, 162–182. [\[CrossRef\]](#)
21. Li, T.; Krumeich, F.; van Bokhoven, J.A. Where Does the Zeolite ZSM-5 Nucleation and Growth Start? The Effect of Aluminum. *Cryst. Growth Des.* **2021**, *19*, 2548–2551. [\[CrossRef\]](#)
22. Yoshioka, T.; Liu, Z.; Iyoki, K.; Chokkalingam, A.; Yonezawa, Y.; Hotta, Y.; Ohnishi, R.; Matsuo, T.; Yanaba, Y.; Ohara, K.; et al. Ultrafast and continuous-flow synthesis of AFX zeolite via interzeolite conversion of FAU zeolite. *React. Chem. Eng.* **2021**, *6*, 74–81. [\[CrossRef\]](#)
23. Yaping, Y.E.; Xiaoqiang, Z.; Weilan, Q.; Mingwen, W. Synthesis of pure zeolites from supersaturated silicon and aluminum alkali extracts from fused coal fly ash. *Fuel* **2008**, *87*, 1880–1886. [\[CrossRef\]](#)
24. De Yoreo, J. A perspective on multistep pathways of nucleation. In *Crystallization via Nonclassical Pathways Volume 1: Nucleation, Assembly, Observation & Application*; American Chemical Society: Washington, DC, USA, 2020; pp. 1–17. [\[CrossRef\]](#)
25. Sheikh, A.Y.; Jones, A.G.; Graham, P. Population balance modeling of particle formation during the chemical synthesis of zeolite crystals: Assessment of hydrothermal precipitation kinetics. *Zeolites* **1996**, *16*, 164–172. [\[CrossRef\]](#)
26. Jorge, M.; Auerbach, S.M.; Monson, P.A. Modelling the thermal stability of precursor nanoparticles in zeolite synthesis. *Mol. Phys.* **2006**, *104*, 3513–3522. [\[CrossRef\]](#)
27. Asselman, K.; Pellens, N.; Thijs, B.; Doppelhammer, N.; Haouas, M.; Taulelle, F.; Martens, J.; Breyhaert, E.; Kirschhock, C.E. Ion-Pairs in Aluminosilicate-Alkali Synthesis Liquids Determine the Aluminum Content and Topology of Crystallizing Zeolites. *Chem. Mater.* **2022**, *34*, 7150–7158. [\[CrossRef\]](#)
28. Kumar, A.; Molinero, V. Two-step to one-step nucleation of a zeolite through a metastable gyroid mesophase. *J. Phys. Chem. Lett.* **2018**, *9*, 5692–5697. [\[CrossRef\]](#)
29. Thompson, R.W. Nucleation, growth, and seeding in zeolite synthesis. In *Verified Syntheses of Zeolitic Materials*; Elsevier: Amsterdam, The Netherlands, 2001; pp. 21–23. [\[CrossRef\]](#)
30. Kumar, M.; Li, R.; Rimer, J.D. Assembly and evolution of amorphous precursors in zeolite L crystallization. *Chem. Mater.* **2016**, *28*, 1714–1727. [\[CrossRef\]](#)
31. Auerbach, S.M.; Ford, M.H.; Monson, P.A. New insights into zeolite formation from molecular modeling. *Curr. Opin. Colloid Interface Sci.* **2005**, *10*, 220–225. [\[CrossRef\]](#)
32. Grand, J.; Awala, H.; Mintova, S. Mechanism of zeolite growth: New findings and open question. *CrystEngComm* **2016**, *18*, 650–664. [\[CrossRef\]](#)

33. Kumar, M.; Choudhary, M.K.; Rimer, J.D. Transient modes of zeolite surface growth from 3D gel-like islands to 2D single layers. *Nat. Commun.* **2018**, *9*, 2129. [\[CrossRef\]](#)
34. Yue, Q.; Kutukova, K.; Li, A.; Čejka, J.; Zschech, E.; Opanasenko, M. Controllable Zeolite AST Crystallization: Between Classical and Reversed Crystal Growth. *Chem.-A Eur. J.* **2022**, *28*, e202200590. [\[CrossRef\]](#)
35. Yao, J.; Huang, Y.; Wang, H. Controlling zeolite structures and morphologies using polymer networks. *J. Mater. Chem.* **2010**, *20*, 9827–9831. [\[CrossRef\]](#)
36. Greer, H.; Wheatley, P.S.; Ashbrook, S.E.; Morris, R.E.; Zhou, W. Early stage reversed crystal growth of zeolite A and its phase transformation to sodalite. *J. Am. Chem. Soc.* **2009**, *131*, 17986–17992. [\[CrossRef\]](#)
37. Boer, D.G.; Asgar Pour, Z.; Langerak, J.; Bakker, B.; Pescarmona, P.P. Binderless Faujasite Beads with Hierarchical Porosity for Selective CO₂ Adsorption for Biogas Upgrading. *Molecules* **2023**, *28*, 2198. [\[CrossRef\]](#)
38. Zhou, W. Reversed crystal growth. *Crystals* **2018**, *9*, 7. [\[CrossRef\]](#)
39. Zhang, X.L.; Qiu, L.F.; Ding, M.Z.; Hu, N.; Zhang, F.; Zhou, R.F.; Chen, X.S.; Kita, H. Preparation of zeolite T membranes by a two-step temperature process for CO₂ separation. *Ind. Eng. Chem. Res.* **2013**, *52*, 16364–16374. [\[CrossRef\]](#)
40. Zhang, X.; Tang, D.; Jiang, G. Synthesis of zeolite NaA at room temperature: The effect of synthesis parameters on crystal size and its size distribution. *Adv. Powder Technol.* **2013**, *24*, 689–696. [\[CrossRef\]](#)
41. Freeman, E.E.; Neeway, J.J.; Motkuri, R.K.; Rimer, J.D.; Mpourmpakis, G. Understanding initial zeolite oligomerization steps with first principles calculations. *AIChE J.* **2020**, *66*, e17107. [\[CrossRef\]](#)
42. Houlléberghs, M.; Breynaert, E.; Asselman, K.; Vaneeckhaute, E.; Radhakrishnan, S.; Anderson, M.W.; Taulelle, F.; Haouas, M.; Martens, J.A.; Kirschhock, C.E. Evolution of the crystal growth mechanism of zeolite W (MER) with temperature. *Microporous Mesoporous Mater.* **2019**, *274*, 379–384. [\[CrossRef\]](#)
43. Chen, H.; Zhang, X.; Zhang, J.; Wang, Q. Controllable synthesis of hierarchical ZSM-5 for hydroconversion of vegetable oil to aviation fuel-like hydrocarbons. *RSC Adv.* **2017**, *7*, 46109–46117. [\[CrossRef\]](#)
44. Xia, Q.-H.; Song, J.; Kawi, S.; Li, L. Characterization and morphological control of β zeolite synthesized in a fluoride medium. *Stud. Surf. Sci. Catal.* **2004**, *154*, 195–202. [\[CrossRef\]](#)
45. Rahman, M.M.; Hasnida, N.; Nik, W.W. Preparation of Zeolite Y Using Local Raw Material Rice Husk as a Silica Source. *J. Sci. Res.* **2009**, *1*, 285–291. [\[CrossRef\]](#)
46. Di Giuseppe, D. Characterization of fibrous mordenite: A first step for the evaluation of its potential toxicity. *Crystals* **2020**, *10*, 769. [\[CrossRef\]](#)
47. Mao, Y.; Zhou, Y.; Wen, H.; Xie, J.; Zhang, W.; Wang, J. Morphology-controlled synthesis of large mordenite crystals. *New J. Chem.* **2014**, *38*, 3295–3301. [\[CrossRef\]](#)
48. Li, J.; Corma, A.; Yu, J. Synthesis of new zeolite structures. *Chem. Soc. Rev.* **2015**, *44*, 7112–7127. [\[CrossRef\]](#)
49. Sánchez, M.; Díaz, R.D.; Córdova, T.; González, G.; Ruetter, F. Study of template interactions in MFI and MEL zeolites using quantum methods. *Microporous Mesoporous Mater.* **2015**, *203*, 91–99. [\[CrossRef\]](#)
50. Cubillas, P.; Stevens, S.M.; Blake, N.; Umemura, A.; Chong, C.B.; Terasaki, O.; Anderson, M.W. AFM and HRSEM investigation of zeolite A crystal growth. Part 1: In the absence of organic additives. *J. Phys. Chem. C* **2011**, *115*, 12567–12574. [\[CrossRef\]](#)
51. Corma, A.; Zones, S.; Čejka, J. *Zeolites and Catalysis: Synthesis, Reactions and Applications*; John Wiley & Sons: Hoboken, NJ, USA, 2010.
52. Smith, R.L.; Sławiński, W.A.; Lind, A.; Wragg, D.S.; Cavka, J.H.; Arstad, B.; Fjellvåg, H.; Attfield, M.P.; Akporiaye, D.; Anderson, M.W. Nanoporous intergrowths: How crystal growth dictates phase composition and hierarchical structure in the CHA/AEI system. *Chem. Mater.* **2015**, *27*, 4205–4215. [\[CrossRef\]](#)
53. John, N.S.; Stevens, S.M.; Terasaki, O.; Anderson, M.W. Evolution of surface morphology with introduction of stacking faults in zeolites. *Chem.-A Eur. J.* **2010**, *16*, 2220–2230. [\[CrossRef\]](#)
54. Li, L.; Lu, Y.; Li, L.; Yang, J.; Fu, W.; Luo, Y.; Lu, J.; Zhang, Y.; Zhou, L. Highly selective zeolite T membranes with different ERI stacking faults for pervaporative dehydration of ethanol. *J. Membr. Sci.* **2021**, *638*, 119701. [\[CrossRef\]](#)
55. Lupulescu, A.I.; Kumar, M.; Rimer, J.D. A facile strategy to design zeolite L crystals with tunable morphology and surface architecture. *J. Am. Chem. Soc.* **2013**, *135*, 6608–6617. [\[CrossRef\]](#)
56. Hould, N.D.; Foster, A.; Lobo, R.F. Zeolite beta mechanisms of nucleation and growth. *Microporous Mesoporous Mater.* **2011**, *142*, 104–115. [\[CrossRef\]](#)
57. Wu, R.; Fan, T.; Chen, J.; Li, Y. Synthetic factors affecting the scalable production of zeolitic imidazolate frameworks. *ACS Sustain. Chem. Eng.* **2019**, *7*, 3632–3646. [\[CrossRef\]](#)
58. Nazari, M.; Yaripour, F.; Shifteh, S. Systematic evaluation and optimization of crystallization conditions for an ethanol-templated ZSM-5 zeolite using response surface methodology. *Adv. Powder Technol.* **2021**, *32*, 4621–4634. [\[CrossRef\]](#)
59. Shamzhy, M.; Opanasenko, M.; Concepción, P.; Martínez, A. New trends in tailoring active sites in zeolite-based catalysts. *Chem. Soc. Rev.* **2019**, *48*, 1095–1149. [\[CrossRef\]](#)
60. Xu, L.; Sun, J. Recent Advances in the Synthesis and Application of Two-Dimensional Zeolites. *Adv. Energy Mater.* **2016**, *6*, 1600441. [\[CrossRef\]](#)
61. Roth, W.J.; Nachtigall, P.; Morris, R.E.; Čejka, J. Two-dimensional zeolites: Current status and perspectives. *Chem. Rev.* **2014**, *114*, 4807–4837. [\[CrossRef\]](#)

62. Přech, J.; Pizarro, P.; Serrano, D.P.; Čejka, J. From 3D to 2D zeolite catalytic materials. *Chem. Soc. Rev.* **2018**, *47*, 8263–8306. [\[CrossRef\]](#)
63. Zhou, W. Microscopic study of crystal defects enriches our knowledge of materials chemistry. *J. Mater. Chem.* **2008**, *18*, 5321–5325. [\[CrossRef\]](#)
64. Wright, P.A.; Zhou, W.; Pérez-Pariente, J.; Arranz, M. Direct observation of growth defects in zeolite beta. *J. Am. Chem. Soc.* **2005**, *127*, 494–495. [\[CrossRef\]](#)
65. Karwacki, L.; Stavitski, E.; Kox, M.H.; Kornatowski, J.; Weckhuysen, B.M. Intergrowth structure of zeolite crystals as determined by optical and fluorescence microscopy of the template-removal process. *Angew. Chem.* **2007**, *119*, 7366–7369. [\[CrossRef\]](#)
66. Silaghi, M.C.; Chizallet, C.; Raybaud, P. Challenges on molecular aspects of dealumination and desilication of zeolites. *Microporous Mesoporous Mater.* **2014**, *191*, 82–96. [\[CrossRef\]](#)
67. Lee, M.J.; Kwon, H.T.; Jeong, H.K. Defect-dependent stability of highly propylene-selective zeolitic-imidazolate framework ZIF-8 membranes. *J. Membr. Sci.* **2017**, *529*, 105–113. [\[CrossRef\]](#)
68. Han, R.; Sholl, D.S. Computational model and characterization of stacking faults in ZIF-8 polymorphs. *J. Phys. Chem. C* **2016**, *120*, 27380–27388. [\[CrossRef\]](#)
69. Deng, A.; Shen, X.; Wan, Z.; Li, Y.; Pang, S.; He, X.; Caro, J.; Huang, A. Elimination of Grain Boundary Defects in Zeolitic Imidazolate Framework ZIF-95 Membrane via Solvent-Free Secondary Growth. *Angew. Chem.* **2021**, *133*, 25667–25671. [\[CrossRef\]](#)
70. Resasco, D.E.; Crossley, S.P.; Wang, B.; White, J.L. Interaction of water with zeolites: A review. *Catal. Rev.* **2021**, *63*, 302–362. [\[CrossRef\]](#)
71. Kumakiri, I.; Sasaki, Y.; Shimidzu, W.; Hashimoto, K.; Kita, H.; Yamaguchi, T.; Nakao, S.I. Micro-structure change of polycrystalline FAU zeolite membranes during a hydrothermal synthesis in a dilute solution. *Microporous Mesoporous Mater.* **2018**, *272*, 53–60. [\[CrossRef\]](#)
72. Anderson, M.W.; Pachis, K.S.; Prébin, F.; Carr, S.W.; Terasaki, O.; Ohsuna, T.; Alfreddson, V. Intergrowths of cubic and hexagonal polytypes of faujasitic zeolites. *Chem. Commun.* **1991**, *23*, 1660–1664. [\[CrossRef\]](#)
73. Catlow, C.R.A.; Sinclair, P.E.; Sokol, A.A. A model for the formation of point defects in zeolites. *Radiat. Eff. Defects Solids* **1999**, *151*, 235–241. [\[CrossRef\]](#)
74. Li, J.; Mayoral, A.; Kubota, Y.; Inagaki, S.; Yu, J.; Terasaki, O. Direct TEM Observation of Vacancy-Mediated Heteroatom Incorporation into a Zeolite Framework: Towards Microscopic Design of Zeolite Catalysts. *Angew. Chem.* **2022**, *134*, e202211196. [\[CrossRef\]](#)
75. Rimer, J.D.; Kumar, M.; Li, R.; Lupulescu, A.I.; Oleksiak, M.D. Tailoring the physicochemical properties of zeolite catalysts. *Catal. Sci. Technol.* **2014**, *4*, 3762–3771. [\[CrossRef\]](#)
76. Dib, E.; Grand, J.; Gedeon, A.; Mintova, S.; Fernandez, C. Control the position of framework defects in zeolites by changing the symmetry of organic structure directing agents. *Microporous Mesoporous Mater.* **2021**, *315*, 110899. [\[CrossRef\]](#)
77. Conroy, B.; Nayak, R.; Hidalgo, A.L.R.; Millar, G.J. Evaluation and application of machine learning principles to Zeolite LTA synthesis. *Microporous Mesoporous Mater.* **2022**, *335*, 111802. [\[CrossRef\]](#)
78. Jensen, Z.; Kim, E.; Kwon, S.; Gani, T.Z.; Román-Leshkov, Y.; Moliner, M.; Corma, A.; Olivetti, E. A machine learning approach to zeolite synthesis enabled by automatic literature data extraction. *ACS Cent. Sci.* **2019**, *5*, 892–899. [\[CrossRef\]](#)
79. Yang, S.; Lach-hab, M.; Vaisman, I.I.; Blaisten-Barojas, E. Identifying zeolite frameworks with a machine learning approach. *J. Phys. Chem. C* **2009**, *113*, 21721–21725. [\[CrossRef\]](#)
80. Ma, S.; Shang, C.; Wang, C.M.; Liu, Z.P. Thermodynamic rules for zeolite formation from machine learning based global optimization. *Chem. Sci.* **2020**, *11*, 10113–10118. [\[CrossRef\]](#)
81. Sebakhy, K.O.; Vitale, G.; Pereira-Almao, P. Production of Highly Dispersed Ni within Nickel Silicate Materials with the MFI Structure for the Selective Hydrogenation of Olefins. *Ind. Eng. Chem. Res.* **2019**, *58*, 8597–8611. [\[CrossRef\]](#)
82. Sebakhy, K.O.; Vitale, G.; Pereira-Almao, P.A. Dispersed Ni-Doped Aegirine Nanocatalysts for the Selective Hydrogenation of Olefinic Molecules. *ACS Appl. Nano Mater* **2018**, *1*, 6269–6280. [\[CrossRef\]](#)
83. El Hariri El Nokab, M. Formation and Structural Analysis of Ultra Low Density Silica Based Aerogels. Master's Thesis, University of Siegen, Siegen, Germany, 2018. [\[CrossRef\]](#)
84. El Hariri El Nokab, M.; Sebakhy, K.O. Solid State NMR Spectroscopy a Valuable Technique for Structural Insights of Advanced Thin Film Materials: A Review. *Nanomaterials* **2022**, *11*, 1494. [\[CrossRef\]](#) [\[PubMed\]](#)

Disclaimer/Publisher's Note: The statements, opinions and data contained in all publications are solely those of the individual author(s) and contributor(s) and not of MDPI and/or the editor(s). MDPI and/or the editor(s) disclaim responsibility for any injury to people or property resulting from any ideas, methods, instructions or products referred to in the content.